The Canadian Mineralogist
Vol. 36, pp. 1327-1338 (1998)

AN UNUSUAL ASSEMBLAGE OF HIGH-Ti OXIDES AND FERROAN CLINOCHLORE ALONG ZONES OF BRITTLE DEFORMATION IN THE VOURINOS (RODIANI) OPHIOLITE COMPLEX, GREECE

GEORGE E. CHRISTIDIS[1]

Department of Mineral Resources Engineering, Technical University of Crete, Chania 73133, Greece

MARIA ECONOMOU-ELIOPOULOS

Department of Geology, University of Athens, Panepistimiopolis, Ano Ilisia, Athens 15784, Greece

THEODOR MARCOPOULOS

Department of Mineral Resources Engineering, Technical University of Crete, Chania 73133, Greece

MAGDA LASKOU

Department of Geology, University of Athens, Panepistimiopolis, Ano Ilisia, Athens 15784, Greece

ABSTRACT

Lenticular bodies of fine-grained light-green chlorite are found at the contact between chromite ore and host serpentinite in the Motsali area of the Vourinos (Rodiani) ophiolite complex, northern Greece. An unusual assemblage of pseudobrookite, the ferrous-iron analogue of pseudobrookite, perovskite, titanite and rutile is present within these bodies. Examination by optical microscopy, electron microprobe, infrared spectroscopy, X-ray fluorescence specroscopy and thermal analysis showed that the original Fe–Ti oxides (pseudobrookite and possibly titanian hematite) and metamorphic clinochlore were converted to an aggregate of fine-grained chlorite with a similar composition, ferroan clinochlore and the ferrous-iron analogue of pseudobrookite. The ferrous-iron analogue of pseudobrookite and perovskite may be associated with rodingite formation, whereas rutile and pseudobrookite, which indicate advanced oxidation of pre-existing Fe–Ti oxides, formed at an earlier stage. The absence of titanian hematite and the formation of the ferrous-iron analogue of pseudobrookite are due to the removal of Fe, which was consumed by the formation of ferroan clinochlore under reducing conditions. The occupancy of the octahedral sites in ferroan clinochlore is controlled by the $^{IV}\mathrm{AlSi}_{-1}$ and the $^{VI}\mathrm{Al}\ (\mathrm{Fe} + \mathrm{Mg})_{-1}$ substitutions, expressed by the total R^{2+} content, *i.e.*, it is represented by the exchange vector $\mathrm{Si}^{VI}\mathrm{Al}\square^{IV}\mathrm{Al}_{-1}R^{2+}_{-2}$, where □ represents a vacancy. Chlorite geothermometry indicates that the association ferrous-iron analogue of pseudobrookite + perovskite + ferroan clinochlore formed at 220–250°C. This inference is consistent with the absence of mixed-layer chlorite – smectite and the observed small size of the chlorite crystals.

Keywords: perovskite, clinochlore, ferrous-iron analogue of pseudobrookite, pseudobrookite, rutile, geothermometer, rodingite, ophiolite, Vourinos (Rodiani), Greece.

SOMMAIRE

Nous décrivons des zones de chlorite vert pâle à grains fins développés le long du contact entre minerai de chromite et la serpentinite hôte, dans la région de Motsali, massif ophiolitique de Vourinos (Rodiani), dans la partie septentrionale de la Grèce. On y trouve un assemblage assez étrange de pseudobrookite, l'analogue riche en Fe^{2+} de la pseudobrookite, pérovskite, titanite et rutile. Nous décrivons cet assemblage par microscopie optique, microsonde électronique, spectroscopie infrarouge, fluorescence X et analyse thermique. Les oxydes de Fe–Ti originaux (pseudobrookite et possiblement hématite titanifère) et le clinochlore métamorphique ont été transformés en agrégat à grains fins de chlorite ayant une composition semblable, un clinochlore riche en fer bivalent, et l'analogue riche en Fe^{2+} de la pseudobrookite. L'analogue riche en Fe^{2+} de la pseudobrookite et la pérovskite pourraient être associées à la formation de la rodingite avoisinante, tandis que rutile et pseudobrookite, qui indiquent une oxydation avancée d'oxydes Fe–Ti pré-existants, se seraient formés à un stade précoce. L'absence d'hématite titanifère et la formation de l'analogue riche en Fe^{2+} de la pseudobrookite seraient dues à la mobilisation du Fe, absorbé par la cristallisation du clinochlore ferreux sous conditions de forte réduction. Le taux d'occupation des sites octaédriques dans le clinochlore ferreux est régi par les schémas de substitution $^{IV}\mathrm{AlSi}_{-1}$ et $^{VI}\mathrm{Al}\ (\mathrm{Fe} + \mathrm{Mg})_{-1}$, exprimés par la teneur totale en R^{2+}, c'est-à-dire, par le vecteur d'échange

---

[1] *E-mail address*: christid@mred.tuc.gr

$\mathrm{Si}^{\mathrm{VI}}\mathrm{Al}\square^{\mathrm{IV}}\mathrm{Al}_{-1}R^{2+}{}_{-2}$, dans lequel □ représente une lacune. La géothermométrie fondée sur la cristallochimie des chlorites montre que l'association de l'analogue riche en Fe^{2+} de la pseudobrookite, perovskite et clinochlore ferreuse s'est formée à 220–250°C. Cette température concorde avec l'absence d'interstratifiés chlorite – smectite et la très petite taille des cristaux de chlorite néoformée.

(Traduit par la Rédaction)

Mots-clés: pérovskite, clinochlore, analogue riche en Fe^{2+} de la pseudobrookite, pseudobrookite, rutile, géothermomètre, rodingite, ophiolite, Vourinos (Rodiani), Grèce.

INTRODUCTION

The Rodiani ophiolitic massif is located 3 km northeast of the Vourinos complex and is tectonically separated from the latter by the Pelagonian basement, which consists mainly of Triassic – Jurassic marble (Brunn 1956). Vourinos is now considered to belong to the supra-subduction zone (SSZ) type of ophiolite (Beccaluva *et al.* 1984), and hosts economically important deposits of chromite (6 million tonnes) (Konstantopoulou & Economou-Eliopoulos 1991). The Rodiani massif has also been exploited for refractory-grade chromite resources (about 250,000 tonnes), but the structural and genetic relationships between the Rodiani massif and the Vourinos complex are not well understood.

Most of the Rodiani rocks consist of serpentinized harzburgite containing bodies of dunite accompanying chromite ore, intruded by pyroxenite, gabbro and rodingitized dykes. Signs of high-temperature deformation superimposed on primary magmatic textures are widespread. In addition, chromite ores and host rocks are strongly deformed, and characterized by foliation, mylonite zones and brittle-shear structures (Economou *et al.* 1986), along which the chromite orebodies are aligned. As a consequence of the brittle tectonism, the metalliferous block near Motsali (Fig. 1) has a brecciated appearance characterized by angular fragments of chromite ore in a rodingite matrix. The matrix consists of hydrogrossular, vesuvianite, epidote and lesser amounts of chlorite and serpentine. Apart from this type of alteration and metamorphism, small (1 m in diameter) lenticular bodies of chlorite are found at the tectonic contact between chromite ore and host serpentinite, in a highly tectonized zone, close to, but not in direct contact with rodingite bodies. Within these chlorite bodies, fine-grained intergrowths of perovskite, two varieties of pseudobrookite, rutile and titanite are present.

Perovskite is a common accessory phase of mantle xenoliths and ultrabasic rocks associated with alkaline silicate and carbonatite magmatism, in which it is primary, *i.e.*, without replacement relationship with associated silicates and magnetite. In some olivinites and clinopyroxenites, it is a cumulate mineral, comprising up to 30 vol.% of the rock (Kukharenko *et al.* 1965). It has also been reported in ultrabasic rocks as a reaction product forming at or above 400°C (Trommsdorff & Evans 1980, Müntener & Hermann 1994) and rodingites (Gekimiantz *et al.* 1996). Preliminary mineralogical and chemical data concerning the presence of perovskite within alteration zones of chromite ores of the Rodiani and Veria areas of northern Greece have been reported by Dimou (1972) and Skounakis (1977). Pseudobrookite has been described in high-grade metapelites and basalts, including lamproites (Rumble 1976, Haggerty 1976, 1991, Brigatti *et al.* 1993). Our purpose in this contribution is a) to examine the textural relationship among chlorite, perovskite, rutile and pseudobrookite, b) to determine the mode of origin of this unusual assemblage, and c) to assess the possible conditions of formation.

MATERIALS

The samples were collected from a lenticular body of chlorite at the contact between a chromite ore and host serpentinite. The material is fine grained, hard, compact, with a light green color and conchoidal fracture, with dark-colored grains of the Ti-bearing phases dispersed throughout its entire mass. It consists of chlorite, which makes up 99 vol.% of the rock, and a multiphase aggregate consisting of Ti-bearing minerals. In contrast to other studies on similar terranes, including the ophiolitic complexes of Greece (Schandl *et al.* 1990, Karkanas 1994), only very minor amounts of titanite were observed. Chlorite is present in three morphologically distinct types: a) relatively coarse-grained chlorite with anomalous interference-colors, the crystals of which display a preferred orientation (type-1 chlorite), b) fine-grained chlorite with a low birefringence, which constitutes more than 95 vol.% of the material (type-2 chlorite), and c) chlorite with a higher birefringence than chlorite of types 1 and 2, which commonly occurs next or close to the Ti-rich assemblage (type-3 chlorite).

EXPERIMENTAL METHODS

The highly compacted material was gently ground, and the particles were dispersed using an ultrasonic bath after addition of Na-polymetaphosphate deflocculant. The less than 2 μm fraction was separated using sedimentation (Moore & Reynolds 1989), after soaking with distilled water overnight. Identification of chlorite was carried out on oriented specimens of the less than 2 μm

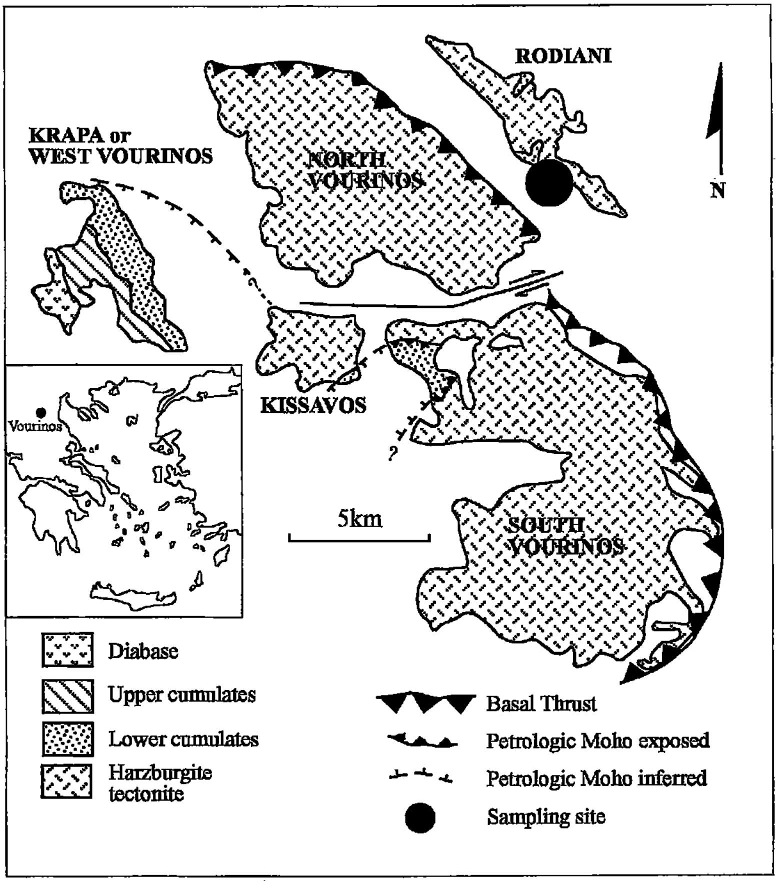

FIG. 1. Location and geological map of the Vourinos ophiolite complex. The study area (Motsali) is indicated with a circle.

fraction by X-ray diffraction (XRD using a Siemens D500 diffractometer, operating at 40 kV and 35 mA, using Ni-filtered Cu*K*α radiation), according to AIPEA recommendations. The polytype of chlorite was determined using the criteria of Bailey (1980) by means of XRD of the bulk samples. Infrared (IR) spectra of chlorite pressed on KBr disks were obtained over the frequency range 200–4000 cm^{-1}, using a Perkin Elmer 883 FTIR spectrometer.

Freshly broken surfaces were examined with a JEOL JSM 540 scanning electron microscope operated at 15 kV, equipped with an Oxford QX 2000 energy-dispersion spectrometer (EDS) for qualitative analysis. Back-scattered electron images were obtained from polished thin sections. The composition of chlorite, pseudobrookite and perovskite was determined by electron-probe micro-analysis (EPMA) using a JEOL 733 Superprobe equipped with a Tracor Northern energy-dispersion spectrometer. The raw spectra were acquired with a focussed beam for 25 s (live time) at an accelerating voltage of 20 kV and a beam current of 3 nA. Measured concentrations were automatically corrected by a ZAF- type correction procedure. The accuracy, precision and detection limits of the method are given in Dunham & Wilkinson (1978).

The structural formulae of the chlorite samples were calculated using 28 atoms of oxygen. Following the reasoning of Hillier & Velde (1991), those compositions with total $Na_2O + K_2O + CaO$ in excess of 0.5 wt% were considered contaminated and were discarded. All Fe was assumed to be Fe^{2+}. The structural formula of the Fe–Ti oxides was calculated using the computer program MINERA14 of Dr. V. Perdikatsis of the Greek Geological Survey (IGME). For "unbalanced" compositions in which totals are lower than 100 wt%, calculation of the amount of ferric iron was performed so as to balance the structural formulae. The program calculates structural formulae of minerals on the basis of both a certain amount of oxygen atoms and a number of cations. The number of ferric iron cations is automatically

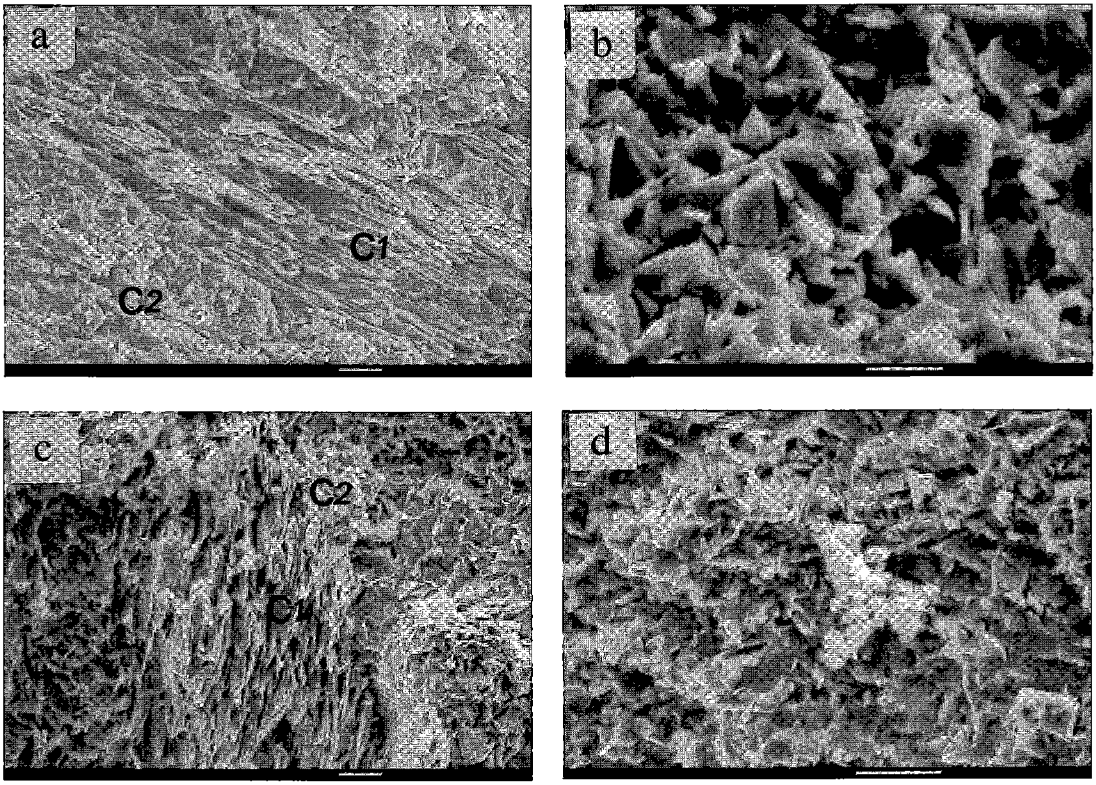

FIG. 2. SEM micrographs of the chlorite-rich material. (a) Elongate crystals of type-1 chlorite (C1) with well-defined boundaries, embedded in a fine-grained groundmass, which consists of type-2 chlorite (C2). (b) Fine silt-size crystals of chlorite (type-2 chlorite), with preferred orientation. (c) Replacement of type-1 chlorite crystals (C1) by type-2 chlorite crystals (C2). (d) White fine-grained crystals of calcite on a fine groundmass of type-2 chlorite crystals. Scale bars: 10 μm in a, c and d, 5 μm in b.

calculated. "Unbalanced" compositions in which the number of cations is not compatible with the required number of oxygen atoms are automatically rejected.

The bulk material was dried at 105°C, ground to pass through a 125-μm sieve, and analyzed for major elements with X-ray fluorescence (XRF), using a Siemens SRS 303 XRF spectrometer. Concentrations of the trace elements, including the rare-earth elements (*REE*), were determined by neutron activation analysis (INAA).

RESULTS

Characterization of chlorite

An XRD analysis revealed the trioctahedral character (d_{060} = 1.5385 Å) and the *IIb* structural type of chlorite. The ethylene glycol saturation of the less than 2 μm fraction did not reveal a swelling component; therefore, within the detection limits of the method, smectite, corrensite and swelling chlorite are not present. The FTIR spectrum of chlorite confirmed the trioctahedral character of the mineral, as indicated by the existence of a significant absorption band at 765 cm^{-1} (Hayashi & Oinuma 1967), which is attributed to Al–O lattice vibrations. The existence of a small absorption band at 3642 cm^{-1}, which has been attributed to the inner OH of the 2:1 layer (Bailey 1988), and which might indicate a significant dioctahedral component (Hayashi & Oinuma 1967), is also common in trioctahedral chlorites (Farmer 1974); it is not incompatible with the trioctahedral character of the mineral.

The SEM examination reveals the presence of small amounts of clay-size crystals of calcite in the chlorite and, in addition, showed that chlorite crystals are in general coarser than 2 μm (Figs. 2a, b). The type-2 and type-3 chlorites consist of crystallites 3 to 5 μm long that cannot be distinguished on the basis of their morphology. Type-1 chlorite consists of larger flakes, longer than 100 μm in places, with considerable variation in size. It occurs in thin linear zones separated from the

TABLE 1. BULK CHEMICAL COMPOSITION OF THE CHLORITE-RICH MATERIAL, VOURINOS (RODIANI) COMPLEX, GREECE

Oxides	Concentration (wt. %)	Trace elements	Concentration (ppm)
SiO_2	32.43	Sc	2.1
TiO_2	0.38	Co	6
Al_2O_3	16.43	Ni	100
Fe_2O_3	1.12	Cr	370
MnO	0.02	Br	1
MgO	36.49		
CaO	0.25		
Na_2O	n.d		
K_2O	0.02		
P_2O_5	0.03		
LOI	13.19		
Total	100.36		

The concentration of the major elements was established by X-ray fluorescence spectroscopy, and that of the trace elements, by instrumental neutron-activation analysis. LOI: loss on ignition; n.d.: not detected. The concentrations of most of the trace elements was found to be below the detection limit of the analytical method. The concentrations of Cr and Ni are typical of those encountered in basic rocks at various occurrences of ophiolite in Greece.

chlorite groundmass by well-defined boundaries (Fig. 2a). These zones are invisible macroscopically. The fine-grained type-2 chlorite replaces type-1 chlorite in places (Fig. 2c), suggesting that its formation took place during a subsequent event. The fine silt-size of the chlorite crystals indicates that the less than 2 μm fraction obtained by sedimentation was produced by crushing of larger grains during sample preparation, *i.e.*, it does not correspond to an actual clay fraction.

The composition of the bulk rock and minerals

The whole-rock chemical composition is given in Table 1. Representative results of the electron-microprobe analyses of the three types of chlorite and the Ti-rich phases are given in Tables 2 and 3, respectively. As expected, the bulk composition of the rock is almost identical to that of the type-1 and type-2 chlorites. Most trace elements, including the *REE*, are present in very low concentrations (below the detection limits of the analytical method). Moreover, the concentrations of Cr, Ni and Co (Table 1) are more typical of metabasic rocks than of serpentinites in ophiolites (Valeton *et al.* 1987, Magganas *et al.* 1991). Therefore, the material may have been formed at the expense of a basic rock (a gabbroic or diabasic dyke), crossing the serpentinized peridotite.

Two varieties of chlorite can be recognized. A homogeneous Mg-rich, Fe-poor variety corresponds to the well-formed and foliated crystals (type-1 chlorite) and to the fine-grained groundmass (type-2 chlorite); it

TABLE 2. REPRESENTATIVE RESULTS OF ELECTRON-MICROPROBE ANALYSES OF CHLORITE-GROUP MINERALS, VOURINOS (RODIANI) COMPLEX, GREECE

	Chlorite type-1 n=14				Chlorite type-2 n=22				Chlorite type-3 n=21			
Oxides (%)	Mean	std	Min	Max	Mean	std	Min	Max	Mean	std	Min	Max
SiO_2	33.20	0.25	32.92	33.78	33.09	0.32	32.07	33.56	30.58	1.36	29.20	33.02
TiO_2	0.04	0.08	0.00	0.19	0.05	0.08	0.00	0.24	0.04	0.07	0.00	0.23
Al_2O_3	16.16	0.13	15.91	16.42	16.47	0.33	15.83	17.15	17.32	1.38	15.53	19.86
Cr_2O_3	--	--	--	--	--	--	--	--	0.21	0.21	0.00	0.65
FeO	0.99	0.09	0.85	1.21	0.91	0.12	0.74	1.17	7.58	2.85	1.53	11.82
MgO	37.13	0.06	36.94	37.23	37.09	0.34	36.52	37.86	29.88	2.81	26.55	36.04
CaO	--	--	--	--	--	--	--	--	0.25	0.24	0.00	0.49
Total	87.52	--	--	--	87.61	--	--	--	85.86	--	--	--
Structural formulae based on 28 oxygens												
Si	6.144	0.029	6.110	6.209	6.115	0.042	6.032	6.179	5.975	0.178	5.614	6.285
Al^{IV}	1.856	0.029	1.791	1.890	1.885	0.042	1.821	1.968	2.025	0.178	1.715	2.386
Al^{VI}	1.666	0.024	1.621	1.698	1.700	0.047	1.613	1.773	1.965	0.201	1.596	2.223
Cr^{3+}	--	--	--	--	--	--	--	--	--	0.033	0.00	0.069
Ti	0.005	0.011	0.00	0.027	0.006	0.011	0.00	0.033	0.005	0.010	0.00	0.034
Fe	0.154	0.014	0.132	0.186	0.141	0.019	0.114	0.181	1.248	0.483	0.216	1.982
Mg	10.246	0.049	10.154	10.314	10.219	0.073	10.010	10.385	8/693	0.621	7.936	10.153
Mg/(Mg+Fe)	0.987	0.005	0.98	0.99	0.988	0.004	0.98	0.99	0.874	0.082	0.80	0.979
Ca	--	--	--	--	--	--	--	--	0.052	0.048	0.00	0.098

n=number of analyses, mean= mean value, std=standard deviation, min= minimum value, max= maximum value. Total iron as FeO and Fe^{2+}.

TABLE 3. CHEMICAL COMPOSITION OF THE Ti- and Fe–Ti-PHASES PRESENT IN THE Ti-BEARING ASSEMBLAGES, VOURINOS (RODIANI) COMPLEX, GREECE

Oxide	Rutile	Perovskite	Pseudobrookite		"Ferro-pseudobrookite"
			1	2	
TiO_2	98.74	57.81	51.24	51.24	69.92
Al_2O_3	n.d	0.19	n.d	n.d	n.d
Cr_2O_3	0.38	n.d	n.d	n.d	0.36
FeO	n.d	0.36	41.47	10.75	27.96
Fe_2O_3	n.d	n.d	- -	34.14	n.d
MnO	n.d	n.d	2.23	2.23	1.03
MgO	n.d	n.d	1.32	1.32	0.78
CaO	0.11	41.11	n.d.	n.d	n.d
Total	99.23	99.47	96.26	99.68	100.22
			Structural formulae		
	4 O atoms	6 O atoms		5 O atoms	5 O atoms
Ti	1.992	1.982	1.667	1.502	2.003
Al	- -	0.010	- -	- -	- -
Cr	0.008	- -	- -	- -	0.011
Fe^{2+}	- -	0.014	1.50	0.349	0.891
Fe^{3+}	- -	- -	- -	1.001	- -
Mn	- -	- -	0.082	0.074	0.033
Mg	- -	- -	0.085	0.077	0.054
Ca	0.003	2.007	-	- -	- -
Cations	2.003	4.013		3.003	3.002

n.d.: not detected. In column 1 under Pseudobrookite, total Fe was calculated as FeO, whereas in column 2, the same total Fe is partitioned between FeO and Fe_2O_3 using the computer program MINERA14. Proportion of oxides reported as wt%.

contrasts with a Fe-enriched variety, close to the Ti-rich phases, characterized by considerable compositional variation (Table 2), and corresponding to the crystals with high birefrigence (type-3 chlorite). Compared to the Mg-rich chlorite, the Fe-enriched variety contains small amounts of Ca and has, on average, less Si and Mg and more Al, which is reflected in the proportion of both the tetrahedrally and octahedrally coordinated Al (Table 2). In spite of the presence of Ca, no swelling component was detected by XRD, probably owing to the small amounts of type-3 chlorite present. Therefore, Ca probably reflects the presence of fine-grained admixtures of calcite (Fig. 2d).

Slight compositional variations are observed in the Fe-poor chlorites; these, however, are not considered statistically significant (Table 2). Type-2 chlorite contains slightly lower amounts of Si, Mg and Fe^{2+}, and a higher amount of Al, in both tetrahedral and octahedral sites, compared to type-1 chlorites. The chemical composition of the type-3 chlorite is dominated by Tschermaks substitution along with $FeMg_{-1}$ and Al_2Mg_{-3} substitution in the octahedral sites (Figs. 3, 4), whereas the $Al_2Fe^{2+}{}_{-3}$ substitution is not significant. Projection of the chlorite compositions in the Al–Mg–Fe^{2+} triangular diagram emphasizes the higher degree of the $FeMg_{-1}$ substitution and the higher Al content of the type-3 chlorite (Fig. 4), whereas chlorites of type 1 and 2 display identical compositions. According to the classification scheme of Hey (1954), all three types of chlorite correspond to clinochlore, with

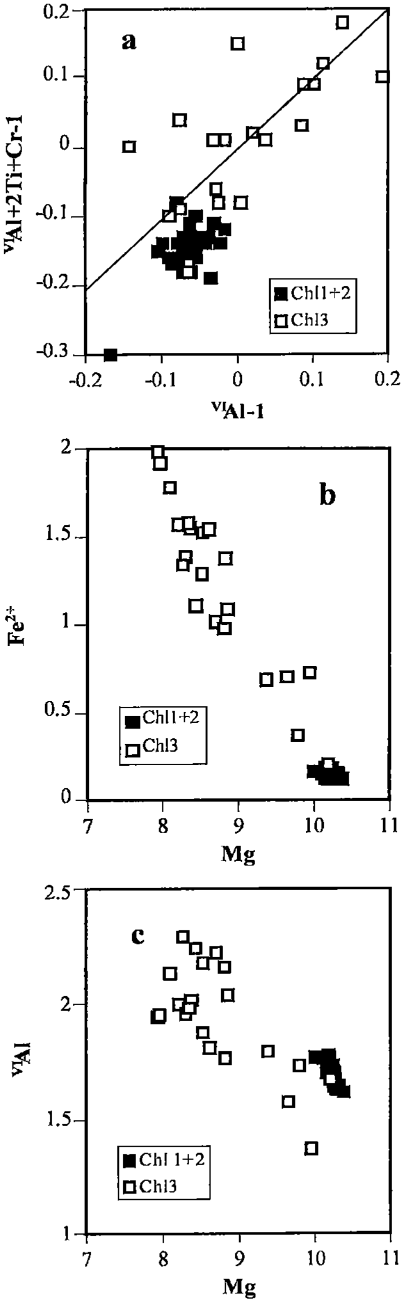

FIG. 3. Factors that control chlorite composition in the material studied. (a) Plot of (^{VI}Al + 2Ti +Cr – 1) *versus* ^{IV}Al – 1, which indicates Tschermak substitution in chlorites (Laird 1988). The Mg-rich chlorites show less Tschermak substitution than ideal clinochlore, like most chlorites present in rodingites and ultramafic rocks. Ferroan clinochlore displays greater Tschermaks substitution than ideal clinochlore, ranging within broad limits. (b) Plot of Mg *versus* Fe, and (c) of Mg *versus* ^{VI}Al. Chl1, Chl2 and Chl3 correspond to type-1, type-2 and type-3 chlorites, respectively.

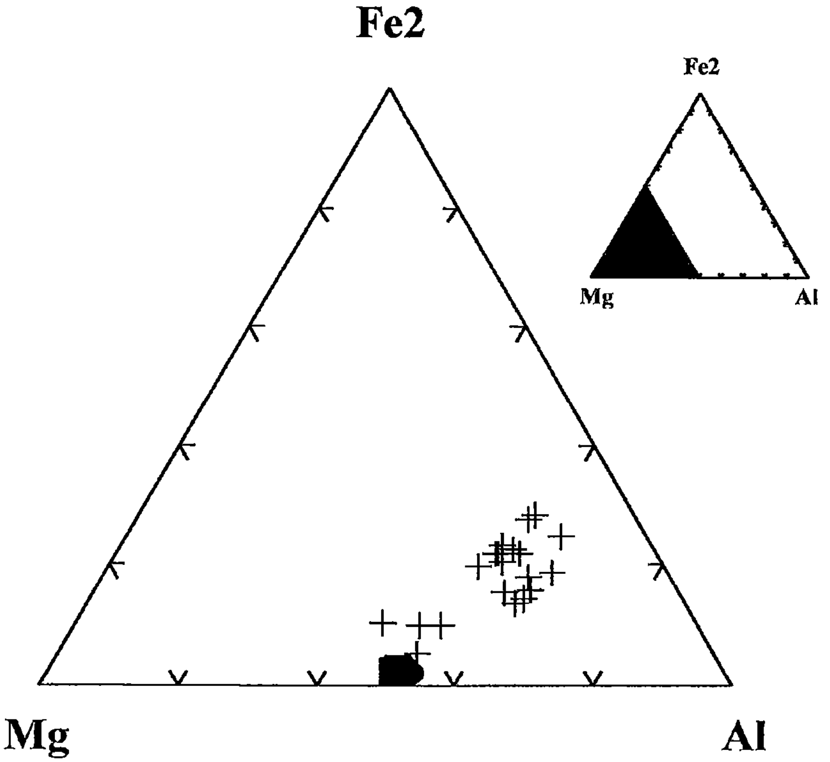

FIG. 4. Chemical composition of chlorites as indicated in the Fe–Al–Mg diagram. Crosses correspond to samples of type-3 chlorite. Note that type-1 and type-2 chlorites plot essentially as a single point.

the chlorite richer in Fe lying close to the border with "pycnochlorite".

The occupancy of the octahedra in all chlorites is close to 12 [on a $O_{20}(OH)_{16}$ basis], suggesting complete occupancy (Fig. 5). Some samples of type-3 chlorite exhibit a slight deficiency at the octahedral sites, ranging from 0.24 to 0.02 atoms per 28 atoms of oxygen (Fig. 6). Owing to the limitations of the analytical method, it is not possible to evaluate the proportion of Fe^{3+}. An attempt to relate occupancy with the excess R^{3+} (Foster 1962) did not reveal a relationship between either the calculated Fe^{3+} content or the total R^{3+} content (including the calculated Fe^{3+} content) and occupancy of the octahedral sites. Instead, it seems that occupancy of the octahedral sites in the type-3 chlorite is related to some degree to Tschermak substitution, since it depends on the $^{IV}\mathrm{AlSi}_{-1}$ substitution and, to a greater extent, on the $^{VI}\mathrm{Al}\,(\mathrm{Fe}+\mathrm{Mg})_{-1}$ substitution, expressed by the total R^{2+} content (Figs. 6a, b). Thus it seems that, where present, occupancy of the octahedral site is controlled by the substitution vector $\mathrm{Si}^{VI}\mathrm{Al}\square^{IV}\mathrm{Al}_{-1}R^{2+}{}_{-2}$, where $\square$ represents a vacancy. Compared with the chlorite of type 3, the occupancy of the octahedra in type-1 and -2 chlorite follows a different trend with respect to the $\mathrm{Si}^{IV}\mathrm{Al}_{-1}$ substitution, but is similar with respect to the $^{VI}\mathrm{Al}\,(\mathrm{Fe}+\mathrm{Mg})_{-1}$ substitution (Figs. 6a, b).

The Ti-bearing assemblage consists of four distinct phases: a Fe–Ti oxide phase, a pure TiO_2 phase corresponding to rutile, a Ti–Ca phase, the chemical composition of which approaches ideal perovskite, and titanite. No ilmenite, titanian magnetite or titanian hematite was identified. The *REE* and alkalis are commonly present in perovskite from alkaline rocks and carbonatites, but are absent here. The lack of the light rare-earths, Na, Sr and Nb distinguishes metamorphic perovskite from that found in alkaline rocks and carbonatite (A.R. Chakhmouradian, pers. commun., 1998). Two distinct Fe–Ti oxides were identified: a Fe-rich and a Ti-rich-, Fe-poor variety. If total Fe is considered ferrous, the Ti-rich variety yields a balanced formula, whereas the Fe-rich variety yields an unbalanced formula, and a low total (anal. 3 and 5, Table 3); it has a considerably lower content of Fe than ilmenite. The low Fe-content of the Fe-rich variety implies either that ferric iron is present, or that rutile is intimately intergrown with a phase richer in Fe, *i.e.*, ilmenite or titanian hematite (Haggerty 1976, anal. no. 49). Although the Fe–Ti phase looks homogeneous in back-scattered electron images, the latter

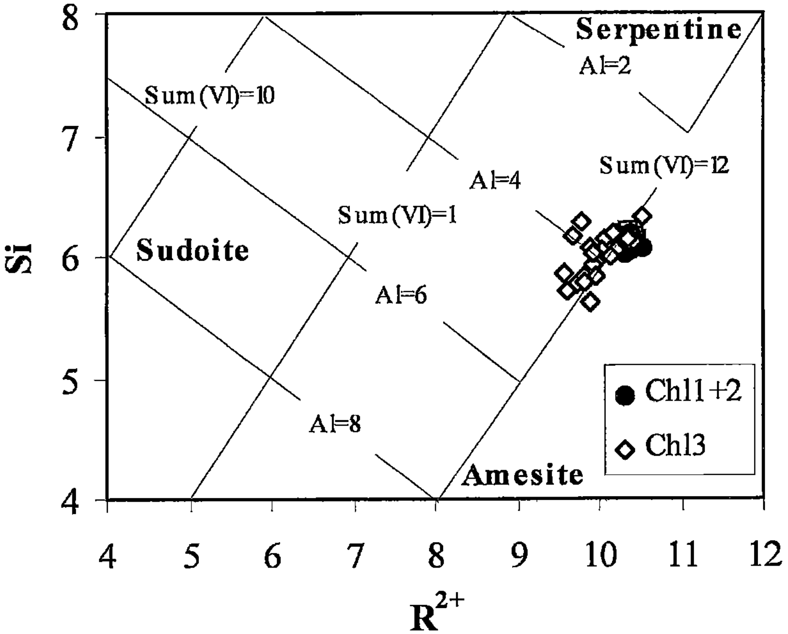

FIG. 5. Projection of the chlorites in the diagram of Wiewióra & Weiss (1990). Note that most chlorites have almost full occupancy of the octahedral sites. Chl1, Chl2 and Chl3 are defined as in Figure 3.

possibility cannot be excluded; further work by high-resolution transmission electron microscopy is needed to clarify this point.

If one allots some of the iron to the ferric state, ("pseudobrookite 2" in Table 3), the Fe-rich phase is found to be pseudobrookite (Haggerty 1976, Bowles 1988), whereas the Ti-rich, Fe-poor variety (70 wt% TiO_2) is the ferrous-iron analogue of pseudobrookite (the ferrous-iron analogue of armalcolite). Both varieties contain minor Mn and Mg. As far as we know, the $FeTi_2O_5$ end-member has not been reported in nature, although pseudobrookite and armalcolite rich in $FeTi_2O_5$ have been described in lamproites and basalts [Otteman & Frenzel (1965), Brigatti *et al.* (1993); see also Haggerty (1987) and Bowles (1988) for a review of terrestrial occurrences of armalcolite and pseudobrookite]. Back-scattered electron images show that pseudobrookite occurs in the form of thin irregular stripes surrounded by the chlorite groundmass, always in contact with patches of rutile, with or without perovskite and titanite (Fig. 7b). The existence of the ferrous-iron analogue of pseudobrookite is characteristic of

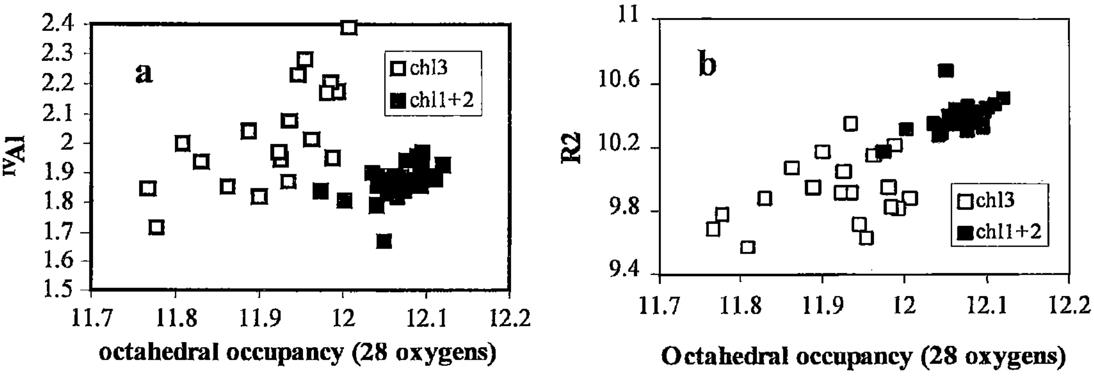

FIG. 6. Factors controlling occupancy of the octahedral sites in the chlorites studied. (a) Plot of ^{IV}Al *versus* occupancy, and (b) plot of R^{2+} *versus* occupancy. Chl1, Chl2 and Chl3 are defined as in Figure 3.

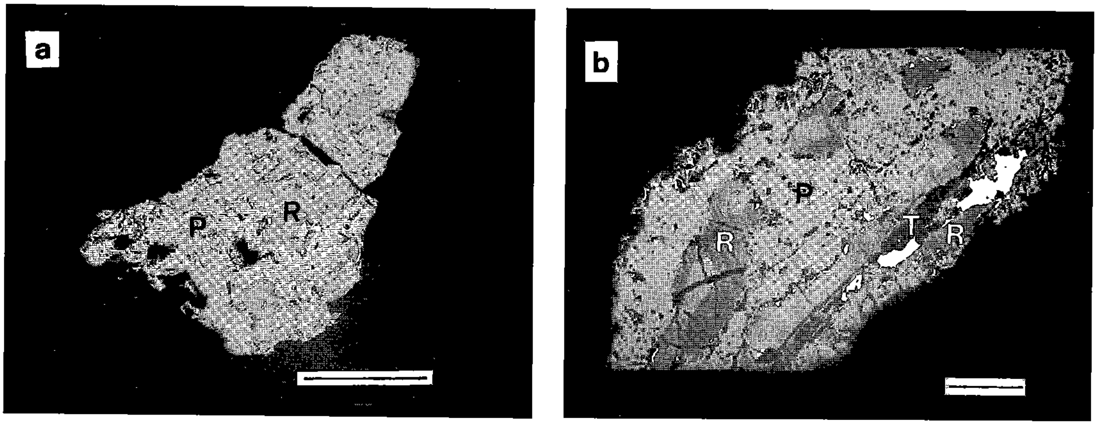

FIG. 7. Back-scattered electron images of the Ti-bearing assemblages. (a) Grey patches of relict crystals of rutile denoted by *R*, surrounded by light grey perovskite, denoted by *P*, suggesting replacement of the former. Scale bar: 100 μm. (b) Dark grey rutile (denoted by *R*) replaced by light grey perovskite (denoted by *P*). Titanite (dark area denoted by T) is closely associated with the ferrous-iron analogue of pseudobrookite (bright area). Scale bar: 10 μm.

extremely reducing conditions (Lindsley 1991). Rutile is surrounded by perovskite, which forms replacement textures (Figs. 7a, b).

DISCUSSION

Relationship between chlorite and Ti-phases

The difference in morphology and the foliation of type-1 chlorite crystals indicate that they formed at a different stage than type-2 and type-3 chlorites. Type-1 chlorite was probably formed during one of the metamorphic events that affected the Vourinos ophiolitic complex (Karkanas 1994). The development of foliation in phyllosilicates in the broader area is associated with oxidation of chromite to ferrian chromite (Economou *et al.* 1986). The replacement textures (Fig. 2c) and the small, uniform size of type-2 chlorite indicate that it replaced type-1 chlorite during a retrograde event at lower temperatures, although it has a slightly higher content of ^{IV}Al (Bailey & Brown 1962, Cathelineau & Nieva 1985, Cathelineau 1988, Hillier & Velde 1991). The small-scale chemical modifications induced by this process include the release of small amounts of Si, Mg and Fe, whereas the slight increase in Al, both as ^{IV}Al and ^{VI}Al, is considered residual.

The close spatial association of type-3 chlorite with the Ti-bearing minerals indicates that its formation is probably related to the alteration of these minerals. Both rutile and pseudobrookite along with titanian hematite are common products of advanced oxidation of titanian magnetite and ilmenite (Haggerty 1976, 1991). Although titanian hematite was not observed, the presence of pseudobrookite and rutile suggests that it might have been present originally, but was subsequently replaced. Oxidation of the original Fe–Ti oxides is believed to have taken place during the brittle deformation of the surrounding rocks and the oxidation of chromite to ferrian chromite and magnetite (M. Economou, unpubl. data).

The absence of titanian hematite and the small amounts of Fe in the Ti-bearing assemblage imply a considerable removal of Fe. Moreover, the existence of the ferrous-iron analogue of pseudobrookite corresponding to the $FeTi_2O_5$ end-member (Table 3), surrounded by rutile and perovskite, suggests reducing conditions. Also, the replacement textures shown in Figure 7 indicate the secondary formation of perovskite after rutile. Therefore, the observed assemblage and its chemical and textural characteristics resulted from a complex process that involved: a) retrograde isochemical recrystallization of type-1 chlorite to type-2 chlorite, b) allochemical conversion of the Fe–Ti-oxide assemblage to the ferrous-iron analogue of pseudobrookite and possibly perovskite, and c) replacement (allochemical) of rutile by perovskite. The Fe released, taken up by magnesian chlorite during the process of retrograde recrystallization, led to ferroan clinochlore (type-3 chlorite) next to the Fe–Ti oxide assemblages. Thus type-2 and type-3 chlorite formed simultaneously, as suggested by the similarity in their morphology, and the difference in their composition was induced by Fe-activity increasing on a microscale. The whole process can be described by the following reaction:

clinochlore + pseudobrookite + titanian hematite (?) + rutile + Ca^{2+} = perovskite + ferroan clinochlore + ferrous-iron analogue of pseudobrookite (1)

The intimate occurrence of titanite and perovskite probably suggests disequilibrium at some point and indicates that the two minerals may not have formed during the same process, but at a later stage from the following reaction:

$$CaTiO_3 + TiO_2 + Ca^{2+} + 2Si^{4+} = CaTiSiO_5 \qquad (2)$$

According to reaction (1), the two varieties of pseudobrookite were formed in separate events, the Ti-rich variety being a product of alteration of the Fe-rich variety in reducing conditions. The difference in chemistry between the type-2 and type-3 chlorites, which formed during a common event, is due to the participation of Fe^{2+} in the latter reaction, whereas the observed increase of Al in type-3 chlorite is residual. The differences in the composition of type-3 chlorite (Table 2) and the compositional trends (Figs. 3–6) are thus principally due to the relative mobility of Fe, which caused chemical gradients during recrystallization of type-1 chlorite. The lack of diffusion haloes (*i.e.*, lack of type-3 chlorite) around several rutile–perovskite grains points to at least partial removal of Fe^{2+} by a fluid phase, which is compatible with the suggestion of a reducing environment during alteration.

The formation of perovskite and titanite suggests that Ca was supplied by a fluid phase. The latter might be associated with the rodingitization observed in the broader area (Karkanas 1994). Chlorite is a common mineral of rodingites, especially those close to the boundary between serpentinite and its host rock, where it forms a "blackwall" (Chidester *et al.* 1978, Schandl *et al.* 1989). Calcium silicate minerals have been reported in rodingites in the nearby area (Dimou 1972, Karkanas 1994), but were not observed in this occurrence. The incomplete replacement of rutile and Fe–Ti-oxides by perovskite, the scarce presence of fine crystals of calcite, and the lack of Ca-silicates typical for rodingites (hydrogrossular, vesuvianite, diopside, prehnite) may be due to the high rate of fluid flow, which flushed Ca out of the system [see Schandl *et al.* (1989) for details]. The Ca removed was probably used up during the formation of Ca-silicates and calcite, which are abundant in the nearby occurrences of rodingite (Karkanas 1994).

TABLE 4. TEMPERATURE OF FORMATION OF THE DIFFERENT TYPES OF CHLORITE BASED ON VARIOUS CHLORITE GEOTHERMOMETERS

Geothermometer		type-2 chlorite	type-3 chlorite
Hillier & Velde (1991)	1	240°C	260°C
Cathelineau (1988)	2	n.a.	265°C
Kranidiotis & MacLean (1987)		219°C	240°C
Jowett (1991)		>500°C	>500°C

1: Geothermometer based on the amount of ^{IV}Al; 2: geothermometer based on the amount of octahedral-site vacancies. n.a. = not applicable.

Temperature of formation of the chlorite, perovskite and the ferrous-iron analogue of pseudobrookite

The extent of Al-for-Si substitution in the tetrahedral sites and the octahedral-site occupancy of chlorites have been used as geothermometers in the temperature range 100°–350°C (Cathelineau & Nieva 1985, Kranidiotis & McLean 1987, Cathelineau 1988, Hillier & Velde 1991, Jowett 1991). In the present study, the observed compositional variation of the type-3 chlorite is attributed to the microenvironmental conditions (*i.e.*, relative mobilization of various elements) and cannot be attributed to variation of temperature, due to the small distance (100–200 μm) over which this variation is observed. Therefore, only the average values of the parameters mentioned could be used for estimation of the temperature of formation of the assemblage type-3 and type-2 chlorite + perovskite + the ferrous-iron analogue of pseudobrookite. The temperatures obtained for the type-2 and type-3 chlorite using the various chlorite geothermometers are listed in Table 4. All geothermometers that yielded reasonable temperatures give higher temperature for the type-3 chlorite due to the higher ^{IV}Al content, although both chlorite types probably formed simultaneously.

The temperatures obtained using the different geothermometers are considered reliable, notwithstanding the drawbacks of empirical geothermometry (de Caritat *et al.* 1993, Essene & Peacor 1995). Note that the possible temperature of formation of the assemblage chlorite, the ferrous-iron analogue of pseudobrookite + perovskite is limited by a number of factors including: a) the absence of swelling chlorite or mixed-layer chlorite–smectite (C/S), usually present in other areas that include rodingites (Bettison & Schiffman 1988, Dubińska 1995, Dubińska *et al.* 1995); b) the temperature at which rodingitization takes place, and c) the fine silt size of the chlorite crystals. The complete conversion of C/S to chlorite has been reported in the temperature range 200–240°C (Kristmannsdottir 1979, Bettison & Schiffman 1988) in hydrothermal environments. Isotopic data indicate that rodingitization occurs in the temperature range 25–400°C (Wenner 1979), and many rodingites form at or below 300°C (*e.g.*, Honnorez & Kirst 1975, Schandl *et al.* 1989, 1990). The fine silt size of type-2 and type-3 chlorites (3–5 μm) indicates that the temperature of their formation should not be much higher than that of the conversion of C/S to chlorite. The fact that the higher ^{IV}Al content of type-3 chlorite is due to element redistribution rather than higher temperature of formation indicates that the temperature of formation of the assemblage ferrous-iron analogue of pseudobrookite, perovskite and type-2 and type-3 chlorites was probably in the range 220–250°C. Such a temperature is low, especially for the ferrous-iron analogue of pseudobrookite, which is stable above 1140°C and under reducing conditions in the laboratory (Lindsley 1991), indicating that the mineral is probably metastable.

ACKNOWLEDGEMENTS

We thank Mr. I. Katsikis and Dr. G. Economou of IGME for their assistance with the electron-probe micro-analyses. The aid of Ms. E. Repouskou from the TUC in the scanning electron microscopy was invaluable. Prof. R. Gieré revised an earlier draft of the manuscript, and S. Haggerty provided significant information about the stability of the ferrous-iron analogue of pseudobrookite. The constructive comments of A. Chakhmouradian, E. Dubińska and the editor improved the text.

REFERENCES

Bailey, S.W. (1980): Structure of layer silicates. *In* Crystals Structures of Clay Minerals and their X-Ray Identification (G.W. Brindley & G. Brown, eds.). Mineralogical Society, London, U.K. (1-124).

________ (1988): Chlorites: structures and crystal chemistry. *In* Hydrous Phyllosilicates (Exclusive of Micas) (S.W. Bailey, ed.). *Rev. Mineral.* **19**, 347-403.

Beccaluva, L., Ohnenstetter, D., Ohnenstetter, M. & Paupy, A. (1984): Two magmatic series with island arc affinities within the Vourinos ophiolite. *Contrib. Mineral. Petrol.* **85**, 253-271.

Bettison, L.A. & Schiffmann, P. (1988): Compositional and structural variations of phyllosilicates from the Point Sal ophiolite, California. *Am. Mineral.* **73**, 62-76.

Bowles, J.F.W. (1988): Definition and range of composition of naturally occurring minerals with the pseudobrookite structure. *Am. Mineral.* **73**, 1377-1383.

Brigatti, M.F., Contini, S., Capedri, S. & Poppi, L. (1993): Crystal chemistry and cation ordering in pseudobrookite and armalcolite from Spanish lamproites. *Eur. J. Mineral.* **5**, 73-84.

Brown, B.E. & Bailey, S.W. (1962): Chlorite polytypism. I. Regular and semi-random one layer structures. *Am. Mineral.* **47**, 819-850.

Brunn, J. (1956): Contribution à l'étude geologique du Pinde Septentrional et d'une partie de la Macédoine Occidentale. *Ann. Géol. Pays Helléniques* **7**, 1-358.

Cathelineau, M. (1988): Cation site occupancy in chlorites and illites as a function of temperature. *Clay Mineral.* **23**, 471-485.

________ & Nieva, D. (1985): A chlorite solid solution geothermometer: the Los Azufres (Mexico) geothermal system. *Contrib. Mineral. Petrol.* **91**, 235-244.

Chidester, A.H., Albee, A.L. & Cady, W.M. (1978): Petrology, structure and genesis of the asbestos-bearing ultramafic rocks of the Belvidere Mountain area in Vermont. *U.S. Geol. Surv., Prof. Pap.* **1016**.

de Caritat, P., Hutcheon, I. & Walshe, J.L. (1993): Chlorite geothermometry: a review. *Clays Clay Minerals* **41**, 219-239.

Dimou, E.G. (1972): About some occurrences of rodingites in Greece. *Bull. Geol. Soc. Greece* **8**, 142-162.

Dubińska, E. (1995): Rodingites of the eastern part of Jordanów–Gogołów serpentinite massif, lower Silesia, Poland. *Can. Mineral.* **33**, 585-608.

________, Bylina, P. & Sakharov, B.A. (1995): Corrensite from Nasławice (Lower Silesia, Poland): some problems of mineral identification and origin. *Clays Clay Minerals* **43**, 630-636.

Dunham , A.C. & Wilkinson, F.C.F. (1978): Accuracy, precision and detection limits of energy dispersive electron-microprobe analyses of silicates. *X-Ray Spectrom.* **7**, 50-56.

Economou, M., Dimou, E., Economou, G., Migiros, G., Vacondios, I., Grivas, E., Rassios, A. & Dabitzias, S. (1986): Chromite deposits of Greece. *In* Metallogeny of Ophiolites, UNESCO IGCP 197 Project (W. Petraschek, S. Karamata, G. Kravchenko, Z. Johan, M. Economou & T. Engin, eds.). Theophrastus, Athens, Greece (129-160).

Essene, E.J. & Peacor, D.R. (1995): Clay mineral thermometry – a critical perspective. *Clays Clay Minerals* **43**, 540-553.

Farmer, V.C. (1974): The layer silicates. *In* The Infrared Spectra of Minerals (V.C. Farmer, ed.). Mineralogical Society, London, U.K. (331-363).

Foster, M.D. (1962): Interpretation of the composition and a classification of the chlorites. *U.S. Geol. Surv., Prof. Pap.* **414-A**, 1-33.

Gekimianitz, V.M., Popov, V.A., Pushcharovsky, D. Yu. & Spiridonov, E.M. (1996): New data on perovskite from the rodingite assemblage, Mineral Mines of South West Urals. Ekaterinburg '96, Summer Mineral School Abstracts (155-160).

Haggerty, S.E. (1976): Oxidation of opaque mineral oxides in basalts. *In* Oxide Minerals (D. Rumble, III, ed.). *Rev. Mineral.* **3**, 1-100.

________ (1987): Metasomatic mineral titanates in upper mantle xenoliths. *In* Mantle Xenoliths (P.H. Nixon ed.). J. Wiley & Sons, New York, N.Y. (671-690).

________ (1991): Oxide textures – a mini atlas. *In* Oxide Minerals: Petrologic and Magnetic Significance (D.H. Lindsley, ed.). *Rev. Mineral.* **25**, 129-219.

Hayashi, H. & Oinuma, K. (1967): Si–O absorption band near 1000 cm^{-1} and OH absorption bands of chlorite. *Am Mineral.* **52**, 1206-1210.

Hey, M.H. (1954): A new review of the chlorites. *Mineral. Mag.* **30**, 277-292.

HILLIER, S. & VELDE, B. (1991): Octahedral occupancy and the chemical composition of diagenetic (low temperature) chlorites. *Clay Mineral.* **26**, 149-168.

HONNOREZ, J. & KIRST, P. (1975): Petrology of rodingites from the Equatorial mid-Atlantic fracture zones and their geotectonic significance. *Contrib. Mineral. Petrol.* **49**, 233-257.

JOWETT, E.C. (1991): Fitting iron and magnesium into the hydrothermal chlorite geothermometer. *Geol. Assoc. Can. – Mineral. Assoc. Can. – Soc. Econ. Geol., Program Abstr.* **16**, A62.

KARKANAS, P. (1994): *Study of the Chrysotile Asbestos Deposit of Zidani, Kozani, and the Occurrence of Tremolite Asbestos of Ano Agoriani, Othrys, Greece.* Ph.D. thesis, Univ. Athens, Athens, Greece.

KONSTANTOPOULOU, G. & ECONOMOU-ELIOPOULOS, M. (1991): Distribution of platinum-group elements and gold within the Vourinos chromitite ores, Greece. *Econ. Geol.* **86**, 1672-1682.

KRANIDIOTIS, P. & MACLEAN, W.H. (1987): Systematics of chlorite alteration at the Phelps Dodge massive sulphide deposit, Matagami, Quebec. *Econ. Geol.* **82**, 1898-1911.

KRISTMANNSDOTTIR, H. (1979): Alteration of basaltic rocks by hydrothermal activity at 100–300°C. *In* Proc. Inter. Clay Conf. 1978 (M.M. Mortland & V.C. Farmer, eds.). Elsevier, Amsterdam, The Netherlands.

KUKHARENKO, A.A., ORLOVA, M.P., BULAKH, A.G., BAGDASANOV, YE.A., RIMSKAYA-KORSAKOVA, O.M., NEFELOV, E.I., ILINSKI, G.A., SERGEEV, A.S. & ABAKUMOVA, N.B. (1965): *The Caledonian Complex of ultramafic-alkaline rocks and carbonatites of the Kola Peninsula and North Karelia.* Nedra Press, Moscow, Russia (in Russ.).

LAIRD, J. (1988): Chlorites: metamorphic petrology. *In* Hydrous Phyllosilicates (Exclusive of Micas) (S.W. Bailey, ed.). *Rev. Mineral.* **19**, 405-453.

LINDSLEY, D.H. (1991): Experimental studies of oxide minerals *In* Oxide Minerals: Petrologic and Magnetic Significance (D.H. Lindsley, ed.). *Rev. Mineral.* **25**, 69-106.

MAGGANAS, A., SIDERIS, C. & KOKKINAKIS, A. (1991): Marginal basin – volcanic arc origin of metabasic rocks of the Circum-Rhodope Belt, Thrace, Greece. *Mineral. Petrol.* **44**, 235-252.

MOORE, D.M. & REYNOLDS, R.C. (1989): *X-Ray Diffraction and the Identification and Analysis of Clay Minerals.* Oxford University Press, Oxford, U.K. (179-201).

MÜNTENER, O. & HERMANN, J. (1994): Titanian andradite in a metapyroxenite layer from the Malenco ultramafics (Italy): implications for Ti-mobility and low oxygen fugacity. *Contrib. Mineral. Petrol.* **116**, 156-168.

OTTEMANN, J. & FRENZEL, G. (1965): Der Chemismus der Pseudobrookite von Vulkaniten. (Eine Untersuchung mit der Electronen-Mikrosonde). *Schweiz. Mineral. Petrol. Mitt.* **45**, 819-836.

RUMBLE, D., III (1976): Oxide minerals in metamorphic rocks. *In* Oxide Minerals (D. Rumble, III, ed.). *Rev. Mineral.* **3**, R1-R20.

SCHANDL, E.S., O'HANLEY, D.S. & WICKS, F.J. (1989): Rodingites in serpentinized ultramafic rocks of the Abitibi greenstone belt, Ontario. *Can Mineral.* **27**, 579-591.

________, ________ & ________ (1990): Fluid inclusions in rodingite: a geothermometer for serpentinization. *Econ. Geol.* **85**, 1273-1276.

SKOUNAKIS, S. (1977): Presence and formation conditions of perovskite in chromitiferous outcrops at Rodiani, Kozani prefecture. *Bull. Geol. Soc. Greece* **13**, 98-103.

TROMMSDORFF, V. & EVANS, B.W. (1980): Titanian hydroxylclinohumite: formation and breakdown in antigorite rocks (Malenco, Italy). *Contrib. Mineral. Petrol.* **72**, 229-242.

VALETON, I., BIERMANN, B., RECHE, R. & ROSENBERG, F. (1987): Genesis of nickel laterites and bauxites in Greece during the Jurassic and Cretaceous, and their relation to ultrabasic parent rocks. *Ore Geol. Rev.* **2**, 359-404.

WENNER, D.B. (1979): Hydrogen, oxygen and carbon isotopic evidence for the origin of rodingites in serpentinized ultramafic rocks. *Geochim. Cosmochim. Acta* **43**, 603-614.

WIEWIÓRA, A. & WEISS, Z. (1990): Crystallochemical classifications of phyllosilicates based on the unified system of projection of chemical composition. II. The chlorite group. *Clay Mineral.* **25**, 83-92.

Received October 10, 1997, revised manuscript accepted November 5, 1998.